Solar Energy Materials & Solar Cells 212 (2020) 110556

Contents lists available at ScienceDirect

Solar Energy Materials and Solar Cells

journal homepage: http://www.elsevier.com/locate/solmat

Novel photoelectrocatalytic/solar cell improvement for organic dye degradation based on simple dip coating $WO_3/BiVO_4$ photoanode electrode

Watcharapong Nareejun [a], Chatchai Ponchio [a,b,*]

[a] Department of Chemistry, Faculty of Science and Technology, Rajamangala University of Technology Thanyaburi, Klong 6, Thanyaburi, Pathum Thani, 12120, Thailand

[b] Advanced Materials Design and Development (AMDD) Research Unit, Faculty of Science and Technology, Rajamangala University of Technology Thanyaburi, Klong 6, Thanyaburi, Pathum Thani, 12110, Thailand

ARTICLE INFO

Keywords:
Photoelectrocatalytic cell
Solar cell
Organic dye degradation
$WO_3/BiVO_4$ thin film
Dip coating method

ABSTRACT

This work focuses on developing a novel photoelectrocatalytic (PEC) cell combined with a solar cell for the highest efficiency, simplest process, and most energy savings to degrade organic dyes in wastewater. FTO/WO_3/$BiVO_4$ photoanode electrode fabrication was developed with the simple layer-by-layer dip coating method, which allows production to be scaled up in the future. The fabricated $WO_3/BiVO_4$ shows thin film properties of high porosity, good visible light absorption, and ability to cover the entire FTO substrate area. The developed FTO/$WO_3/BiVO_4$ electrode exhibits high oxidation activity and high durability, and it can be applied to the PEC cell prototype by working under the catalytic mechanism of light irradiation and bias potential for organic dye degradation. The novel PEC cell was especially designed to include a solar cell to convert light into electrical energy that is stored in batteries for potential bias at the anode electrode and to supply electricity to the light-irradiated electrode and solar cell panel under the electrical circuit's controller. The result shows that the developed PEC cell prototype can operate on its own without using external power and is able to degrade methylene blue and rhodamine B dyes up to 94% and 93% in 3 h, respectively. This research provides a novel, innovative PEC cell prototype that is highly effective at removing various organic dye substances, uses a simple method, offers an energy saving process, and is a very interesting way to further a large industrial dye wastewater treatment system.

1. Introduction

Organic dyes from industrial systems make it necessary to accelerate the development of removal techniques because these substances cause water pollution and unsightly scenery [1–5]. Many methods have been developed to treat dye wastewater, such as using chemical coagulation [6–8], membrane [9,10], and biological systems [11,12], but these techniques are still not very effective or compatible methods because they use many removal steps. Therefore, highly effective treatment techniques and simple treatment procedures are urgently needed to solve the previous methods' limitations. The photoelectrocatalytic technique is an attractive method that has many advantages in treating dye wastewater with a highly efficient technique and simple procedures [13–18]. The photoelectrocatalytic cell can be developed by electrode fabrication method improvement [19–22] and photoelectrocatalytic cell designation [23–25] to be a highly effective and practical application. Photoanode electrode development widely uses titanium dioxide (TiO_2) semiconductors because they present high photocatalytic activity under ultraviolet light and are also durable in the environment [26–28]. However, TiO_2 is only active in ultraviolet light that is minimal compared to the visible light in natural light. Therefore, light absorption properties of TiO_2 must increase by the addition of other substances with optical absorption properties in visible light [29–32] or one must select other semiconductors with narrow bandgap energy [33–35]. Tungsten oxide (WO_3) and Bismuth vanadate ($BiVO_4$) are usually selected as narrow semiconductors because they have high photocatalytic activity under visible light region [36–40]. In previous research, we successfully developed composited $WO_3/BiVO_4$ preparation using the spin coating method for water oxidation and organic dye removal under visible light [16,38,41]; however, it was used in a small-scale laboratory application.

* Corresponding author. Department of Chemistry, Faculty of Science and Technology, Rajamangala University of Technology Thanyaburi, Klong 6, Thanyaburi, Pathum Thani, 12120, Thailand.
E-mail address: chatchai@rmutt.ac.th (C. Ponchio).

https://doi.org/10.1016/j.solmat.2020.110556
Received 20 January 2020; Received in revised form 10 March 2020; Accepted 3 April 2020

Therefore, a large-scale and practical electrode preparation process must be studied and developed for industrial plant application. The dip coating technique is one of the simplest techniques that it is still being continuously developed for large-scale thin film fabrication [22,42–45]. The photoelectrocatalytic cell design is especially important for high efficiency, compatibility, and energy saving when applied to a real wastewater treatment system [25,46,47].

In this work we developed the $WO_3/BiVO_4$ photoanode electrode preparation by simple dip-coating method and applied the designed photoelectrocatalytic cell for organic dye degradation. Moreover, a solar cell system and batteries were included to convert light energy into an electrical energy storage system. The results show that the developed system can be applied to the removal of various organic dyes with high efficiency and energy saving process.

2. Experiment

2.1. $WO_3/BiVO_4$ photoanode electrode preparation

A precursor solution of 0.1 M $BiVO_4$ was prepared by mixing 25 ml of 0.2 M $(BiNO_3)_3$ in acetic acid solution with 25 ml of 0.2 M ($C_{10}H_{14}O_5V$) in acetyl acetone solution. 0.1 M WO_3 was prepared by dissolving tungstic acid in 30% ammonia (NH_4OH) solution then refluxed at 60 °C for 1 h. Fluorine doped tin oxide (FTO) 10 × 10 cm in size was used as an electrode substrate. The FTO substrate was cleaned and its surface modified by sonicating in the priority solution of 0.5 M NaOH for 15 min, ethanol for 15 min, and deionized water for 15 min. The modified FTO substrate was dipped in 0.1 M WO_3 solution in the first layer and dried at 150 °C for 5 min. The FTO/WO_3 was dipped in 0.1 M $BiVO_4$ in the second layer and dried again. The FTO/WO_3/$BiVO_4$ was calcined at 550 °C for 1 h and then connected with copper wire and covered by epoxy resin to control the reaction surface area.

2.2. Characterization and photoelectrocatalytic properties analysis

The fabricated FTO/WO_3/$BiVO_4$ was characterized to study the optical property, morphology, chemical composition, and crystalline structure. Absorption property was studied using a UV/Vis spectrophotometer (Shimadzu, UV-1601). The surface morphology of FTO/WO_3/$BiVO_4$ thin film was investigated using an atomic force microscope (AFM) (JEOL, JAFM 4500 XT) and scanning electron microscopy (SEM) (JEOL, JSM 6510). The elemental composition and oxidation states of WO_3 and $BiVO_4$ thin films were confirmed using X-ray photoelectron spectroscopy (XPS) (JEOL, JPS-9010TR). The crystalline structure of $WO_3/BiVO_4$ thin films on the FTO substrate was studied by X-ray diffraction (XRD) (JEOL, JDX-3530) in the 2θ range from 10° to 70°. The photoelectrocatalytic activity for water oxidation was studied using a voltammetry analyser (Princeton Applied Research, Inc., VersaSTAT 3) in a 0.1 M Na_2SO_4 electrolyte solution at an applied potential of 1.0 V versus Ag/AgCl under visible-light illumination. The photoelectrocatalytic organic dye degradation efficiency was studied in 5.0 mg L^{-1} Rhodamine B (RhB) and methylene blue (MB) in a 0.1 M Na_2SO_4 solution under an applied potential of 1.0 V and visible-light irradiation. The concentrations of RhB and MB organic dyes were determined using a UV/Vis spectrophotometer (Shimadzu, UV-2401PC). The following equation calculated organic dye degradation efficiency:

$$\text{Organic dyes degradation}(\%) = \left(\frac{A_0 - A_t}{A_0}\right) \text{x}100 \quad (1)$$

where A_0 is the initial absorbance of organic dyes and A_t is the absorbance of organic dyes at given time t. Moreover, the chemical oxygen demand (COD) parameter was observed to confirm the PEC cell's degradation efficiency.

2.3. PEC cell design

Fig. 1 shows the designed PEC cell including the solar cell system. The PEC cell consists of the developed $WO_3/BiVO_4$ photoanode electrode (1), which was placed parallel to the stainless steel cathode electrode (2). All electrodes were dipped in a 5.0 mg/L MB or RhB solution used as an organic dye sample (3). The cell design included a pump (4) to continuously flow the organic dye solution through the anode electrode (1) and refresh the electrode surface at all time. The system's operation accelerates the reaction at the anode electrode by the light irradiation from 2 lamps (5). The first lamp is located at the anode electrode to accelerate the semiconductor electrode (photocatalysis), and the second lamp is located at the solar cell panel (6) to convert the light energy into electrical energy and charge the battery (7). The battery is responsible for supplying voltage to the lamps (5) and electrodes (1, 2), which control the power supply with the circuit board (8). The circuit board (8) controls the electrical circuit from the solar cells to store electricity in the battery and control the power supply from the battery to the lamps (5) and the electrodes (1, 2). In particular, we control the electric potential at the electrode by adding a voltage control panel device (9) to control the voltage at the electrode so it is specific and constant.

3. Results and discussion

3.1. $WO_3/BiVO_4$ electrode fabrication and characterization

This research has successfully developed $WO_3/BiVO_4$ thin film fabrication on the FTO substrate by a simple dip-coating technique. The inset in Fig. 2b shows the dark-yellow black of $WO_3/BiVO_4$ after calcination at 550 °C, corresponding to the colour of WO_3 and $BiVO_4$ semiconductors [19,41,48]. The $WO_3/BiVO_4$ thin film fabricated by the dip-coating technique presents better homogeneous thin film cover over all areas of the FTO substrate than that the previous spin-coating technique [41]. Fig. 2 shows the higher visible light absorption intensity of $WO_3/BiVO_4$ thin film prepared by the dip coating technique than the spin coating technique due to the effect of thin film coverage on the substrate mentioned above. The inset of Fig. 2a shows the correlation between the absorbance coefficient and bandgap energy (Eg), which could be calculated as 2.40 eV and 2.8 eV, corresponding with $BiVO_4$ and WO_3 at the electrode surface, respectively [16,33,37,49]. The result confirms that both $BiVO_4$ and WO_3 semiconductors can generate hole (h^+) for oxidation reaction efficiently from e^--h^+ charge separation under visible light irradiation. The absorption result confirms that WO_3 in the inner layer can generate e^--h^+ under light irradiation and act as electron separation of the generated electron from the $BiVO_4$ conduction band to the electrode, preventing the charge recombination effect and resulting in improved photoelectrocatalytic activities. Our method improves on previous works that addressed FTO/WO_3/$BiVO_4$ fabricated using the spin coating method [41]. $BiVO_4$ at the outer layer improves visible light absorption and enhances the generated h^+ separation from the valence band of WO_3, which causes highly efficient h^+ to occur and improves the oxidation reaction at the electrode surface. This absorption property indicates that the developed $WO_3/BiVO_4$ thin film electrode has a suitable bandgap for photoelectrocatalytic degradation of organic dye under visible light irradiation [50–53]. Fig. 3(A and B) shows the top view morphology of $WO_3/BiVO_4$ thin film analysis by AFM and SEM techniques with the small particle size of 100–200 nm and present high surface roughness, which places the surface area in contact with organic substances and water for high efficiency of the oxidizing process at the electrode surface. The XPS analysis confirmed the chemical composition and oxidation state of elements on the FTO/WO_3/$BiVO_4$ prepared by dip-coating technique very well. Fig. 4 shows Vanadium ($2p_{3/2}$) and Bismuth ($4f_{7/2}$, $4f_{5/2}$) peaks at the binding energy of 516.5, 158.9, and 164.2 eV, which confirms the chemical composition of thin films with V^{5+} and Bi^{3+} of $BiVO_4$ [54]. In addition, we found the W ($4f_{7/2}$, $4f_{5/2}$)

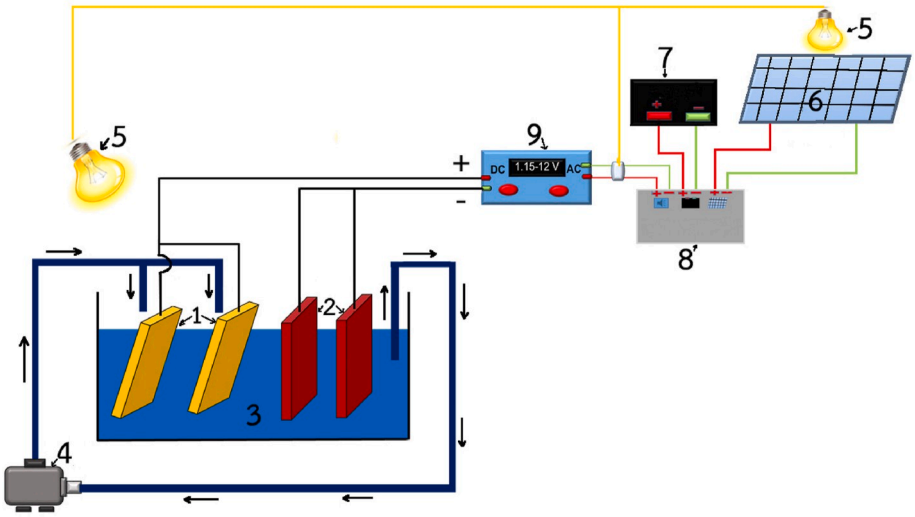

Fig. 1. Schematic PEC cell design including solar cell system (1) FTO/WO_3/$BiVO_4$ anode electrode, (2) stainless steel cathode electrode, (3) organic dyes solution, (4) pump, (5) light sources, (6) solar cell, (7) battery, (8) circuit board, and (9) voltage control panel.

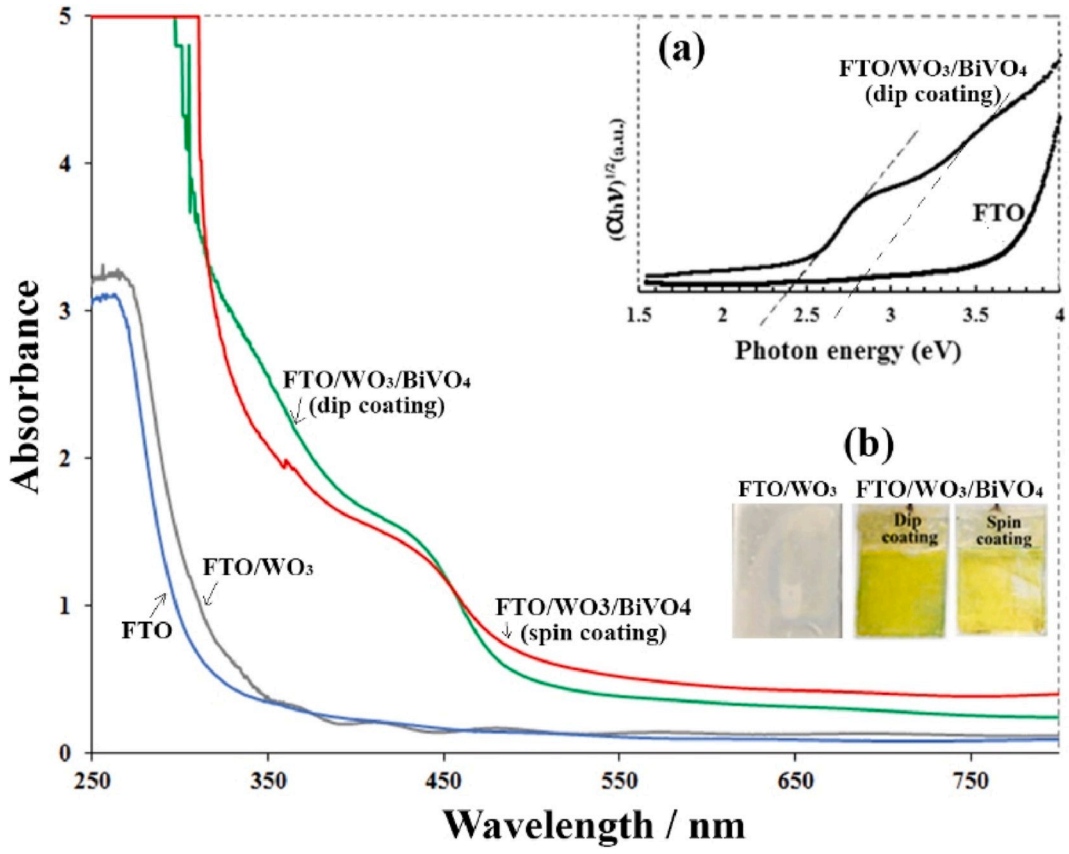

Fig. 2. UV/Vis absorption spectra of FTO substrate, FTO/WO_3, and FTO/WO_3/$BiVO_4$ prepared by dip coating and spin coating techniques. Inset of (a) shows the correlation between the absorbance coefficient and bandgap energy of FTO and FTO/WO_3/$BiVO_4$ prepared by dip coating technique and (b) shows the colour of FTO/WO_3 and FTO/WO_3/$BiVO_4$ thin film prepared by spin coating and dip coating techniques.

peaks at the binding energy of 35.1 and 37.2 eV, which confirms the chemical composition of the thin film has W^{6+} of WO_3 [55,56]. Furthermore, oxygen (1s) is present at the binding energy of 529.8 eV, which means oxygen in the crystal structure of WO_3 and $BiVO_4$ [57,58]. The crystal structure of the FTO/WO_3/$BiVO_4$ electrode prepared by the dip coating technique after it was calcined at 550 °C was studied using X-ray diffraction (XRD). Fig. 5 shows the XRD pattern at 2-theta of 24° that related to monoclinic WO_3 [59], while the monoclinic $BiVO_4$ presents the XRD pattern at 2-theta of 18.8°, 28.9°, and 30.6° [60], respectively. Such studies can confirm that WO_3 and $BiVO_4$ semiconductors are actually on the electrode and have a crystal structure suitable for use as a photocatalytic semiconductor on the electrode for further high oxidation activity of organic dyes. Overall, the characterization confirms the optical properties, morphologies, chemical

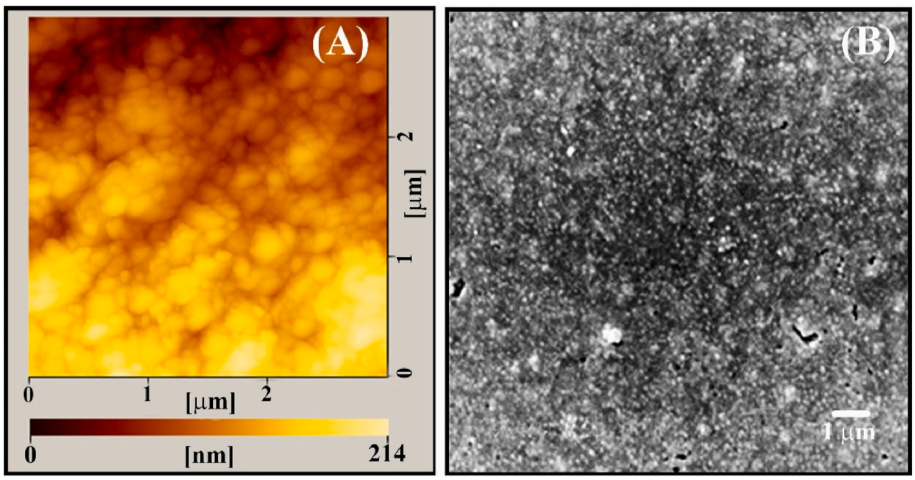

Fig. 3. (A) AFM images and (B) SEM image on the top sectional view images of the fabricated $WO_3/BiVO_4$ thin film on FTO substrate using dip coating technique.

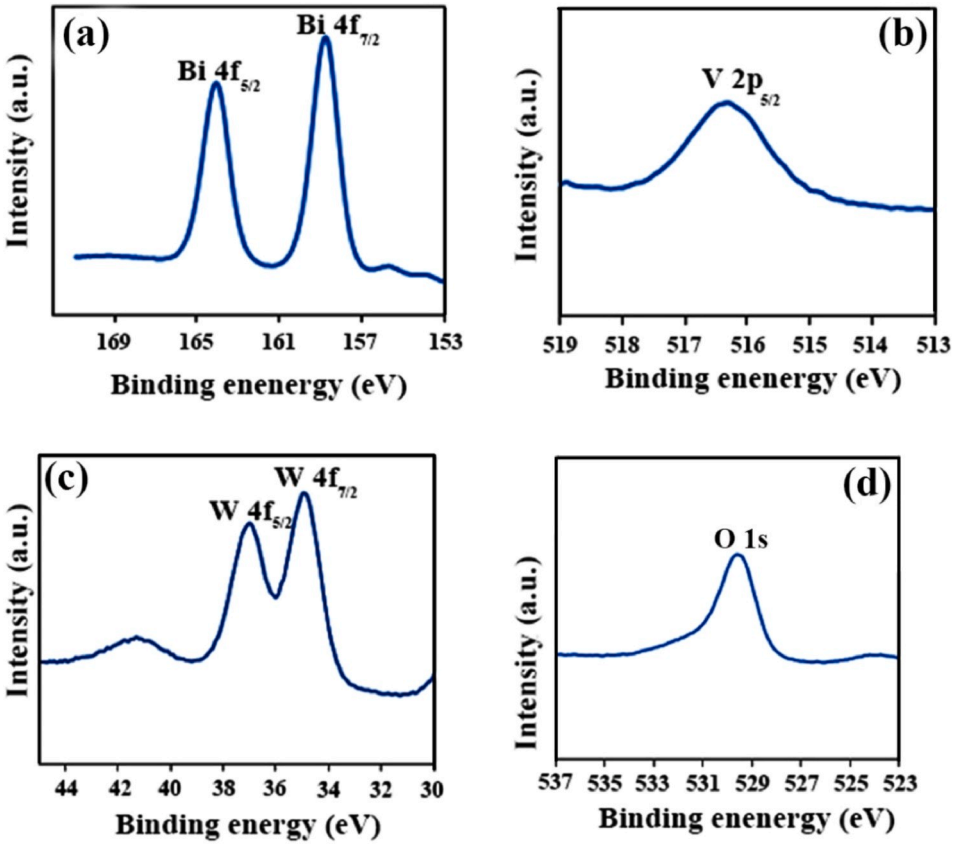

Fig. 4. XPS spectra of (a) Bi 4f, (b) V 2p, (c) W 4f, and (d) O 1s on FTO/WO_3/$BiVO_4$ electrode fabricated by dip coating technique.

composition, and crystalline structure of the fabricated FTO/WO_3/-$BiVO_4$ electrode using the simple method, which was suitably applied to a photoanode electrode in a PEC cell for the dye degradation process.

3.2. Photoelectrocatalytic properties analysis

Fig. 6 shows the anodic photocurrent from the water oxidation process using the $WO_3/BiVO_4$ electrode prepared by the developed dip-coating technique was significantly higher than the previous spin coating technique [41]. The higher photoelectrocatalytic activities of the dip coating technique for $WO_3/BiVO_4$ thin film preparation were consistent with the better physical and absorptive properties compared to the spin coating technique. Importantly, the dip coating technique is also simple and can scale up thin film fabrication better than the spin coating technique, and it is suitable for application to the removal of large-scale dye wastewater.

3.3. The designed PEC cell efficiency for dye degradation

As shown in Fig. 7, the PEC cell design (which includes a solar cell system) was successfully applied to dye degradation under the consideration of the most effective dye removal. Under the optimum condition using parallel FTO/WO_3/$BiVO_4$ photoanode electrodes and the stainless steel cathode electrode with a bias potential of 2.0 V, adjusting the pH

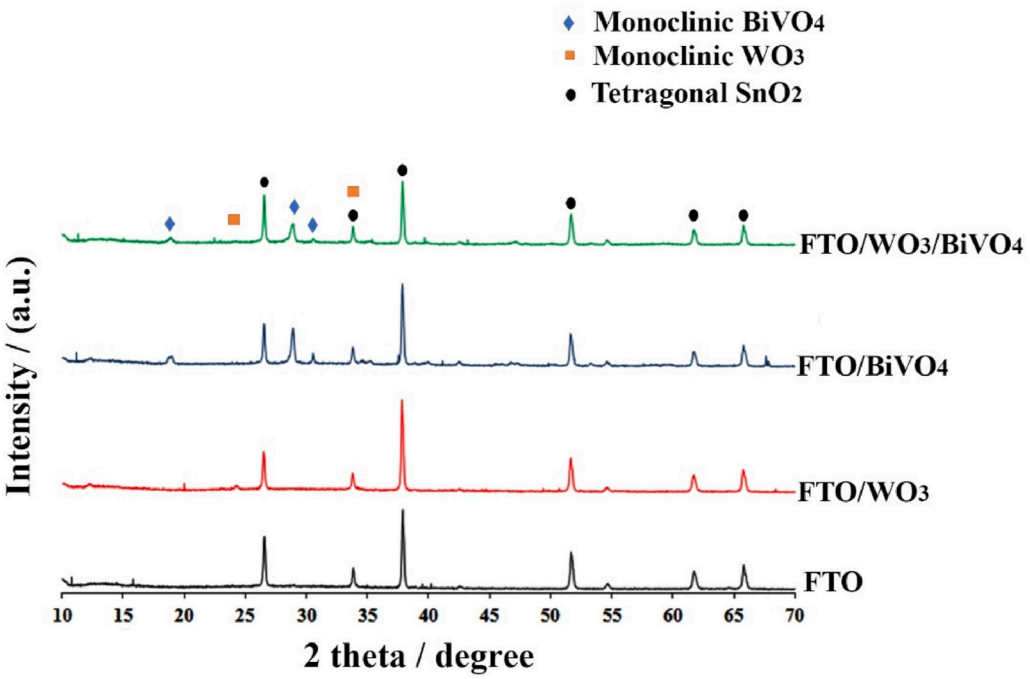

Fig. 5. X-ray diffraction patterns of FTO substrate, FTO/WO_3, FTO/$BiVO_4$ and FTO/WO_3/$BiVO_4$ prepared by dip coating techniques.

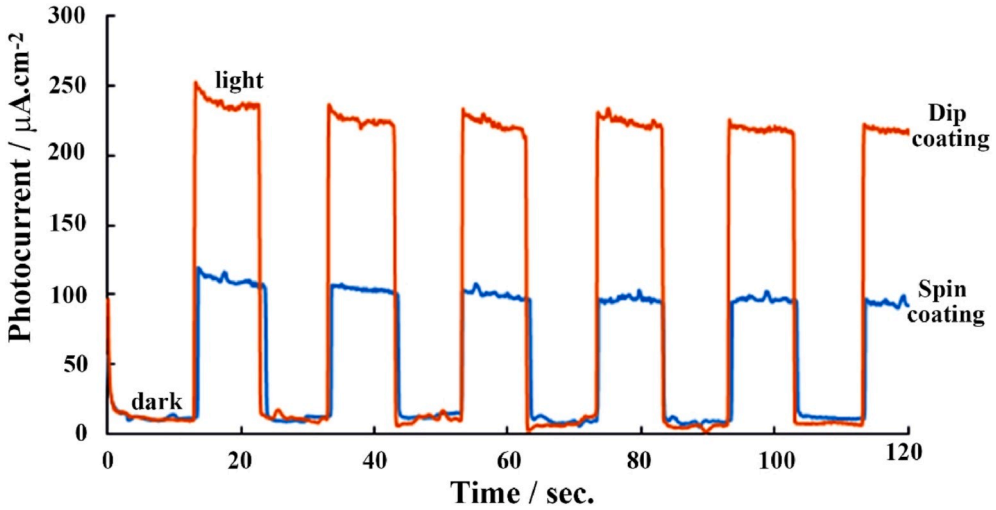

Fig. 6. Photocurrent of FTO/WO_3/$BiVO_4$ electrode with different fabrication of dip coating and spin coating techniques at 1.0 V vs. Ag/AgCl in 0.1 M Na_2SO_4 aqueous solution under periodical visible light irradiation.

value to 3 under 20 W visible light-accelerated conditions in the 10 L dye wastewater container can remove up to 94% and 93% of MB and RhB dye wastewater, respectively, in 3 h as shown in Fig. 8. The inset of Fig. 8 shows the dyes' significant colour change from dark blue and dark pink until it becomes a clear solution, which confirms the high efficiency of the developed PEC cell for dye degradation applications. The COD value was monitored to confirm that the organic dye removal can be changed from the dye substance into CO_2 and H_2O without turning into other organic substances. The result shows that the develop PEC cell can reduce the COD value up to 82% in 180 min, which confirms that the designed PEC cell is highly effective in treating dye wastewater, as shown in Fig. 9. Table 1 shows the dye degradation efficiency improvement of this work compared with the related research. There are presents the % colour degradation of dye up to over 90% for all research. The highlight of this research is higher efficiency COD removal in a shorter time using a light source with lower power than other studies and that can degrade many types of dyes. The developed PEC cell can be used in large-scale applications and save more energy when combined with solar cells. Therefore, we can confirm the high efficiency in large-scale applications and energy-saving of the developed PEC cell for dye degradation. The organic dye removal efficiency on the electrode surface was analysed using the photocatalytic (PC), electrocatalytic (EC), and photoelectrocatalytic (PEC) mechanisms by comparing the percentage of RhB degradation. Fig. 10 shows that the PEC catalytic mechanism has the best dye removal efficiency over EC and PC. The result confirms that both light and applied potential are important factors for the dye degradation efficiency of the developed FTO/WO_3/$BiVO_4$ electrode. Fig. 11 shows a schematic diagram of the reaction on the surface of the FTO/WO_3/$BiVO_4$ electrode under the catalytic condition by light irradiation and bias potential. The separated e^- and h^+ were generated at the conduction band (CB) and valent band (VB) of the WO_3 and $BiVO_4$ semiconductors. The e^- generated at the CB of the

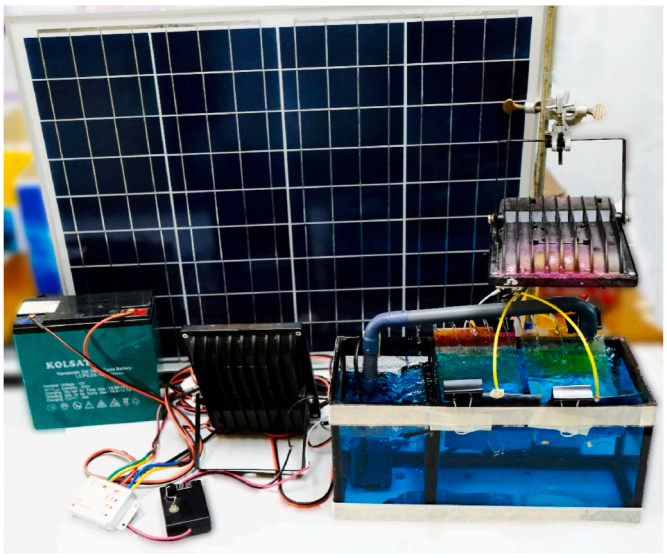

Fig. 7. Experimental set up of the designed PEC cell for dye degradation process.

$BiVO_4$ layer was separated from the CB of the WO_3 layer and transferred to the anode electrode under positive bias potential, which helps reduce the recombination effect of e^- and h^+ of both semiconductors. At the same time, the h^+ generated at the VB position of both semiconductors was separated and transferred from the VB layer of WO_3 to the VB of $BiVO_4$, resulting in many h^+ occurring at the surface of the FTO/WO_3/$BiVO_4$ electrode. The amount of h^+ at the VB of the $BiVO_4$ semiconductor that has high positive potential is sufficient to oxidize various substances on the electrode surface, including water and various organic dye substances at the electrode surface, which confirms the FTO/WO_3/$BiVO_4$ electrode's improvement of the photoelectrocatalytic activities for dye degradation. The results demonstrated that the designed PEC cell is highly effective in removing various dyes in a short time. In addition, the PEC cell cooperating with a solar cell to generate electric support with light and an applied potential system allows the system to work day and night without wasting energy. The designed system is able to work efficiently and is suitable for further application in industrial systems.

4. Conclusions

The designed PEC cell prototype combined with solar cells exhibits high efficiency for various organic dye degradation using a simple fabricated FTO/WO_3/$BiVO_4$ photoanode electrode. The developed FTO/WO_3/$BiVO_4$ electrode using the dip coating method showed higher

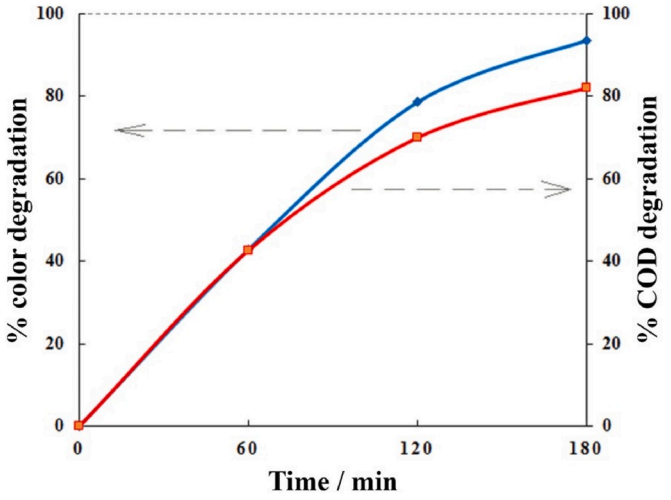

Fig. 9. % Colour and % chemical oxygen demand degradation of Rhodamine B dye by the PEC cell.

Table 1
Efficiency of dye degradation, comparing this work and the related research.

Author/ References	condition	% colour degradation	% organic removal
This work	FTO/WO_3/$BiVO_4$ under 20 W visible light irradiation at an applied potential of 2.0 V for 10,000 mL of dye MB and RhB solution.	94% for 180 min	82% COD removal for 180 min
D. Liu et al., 2017 [61]	FTO/TiO_2 under 450W visible light irradiation at an applied potential of 1.4 V for 50 mL of MB solution	92.9% for 240 min	62% TOC removal for 240 min
Y.M. Hunge et al., 2018 [34]	FTO/WO_3 under 500W visible light irradiation at an applied potential of 1.5 V for 40 mL of brilliant blue solution	92.0% for 240 min	79.5% COD removal for 240 min
R.D. Suryavanshi et al., 2018 [62]	FTO/WO_3/$BiVO_4$ under 300W visible light irradiation at an applied potential of 1.35 V for 100 mL of methylene blue (MB) and Congo red (CR) solution	98% for 180 min	53% TOC removal for 180 min

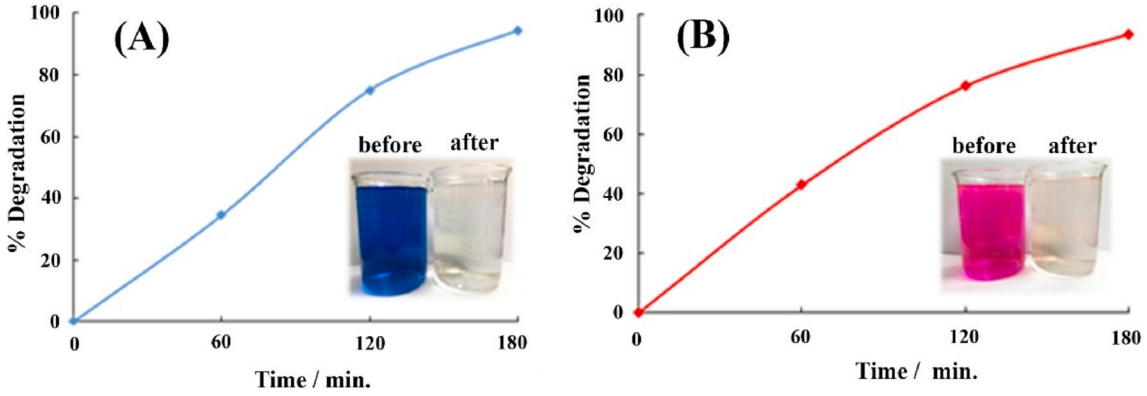

Fig. 8. % Dye degradation of (A) methylene blue and (B) Rhodamine B. The inset shows the colour change of dye before and after the process using the developed PEC cell.

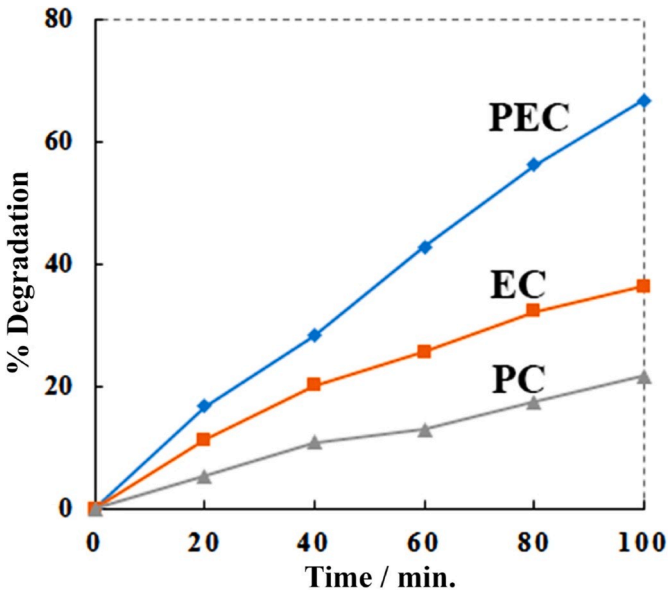

Fig. 10. % Methylene blue dye degradation using photocatalytic (PC), electrocatalytic (EC), and photoelectrocatalytic (PEC) mechanisms.

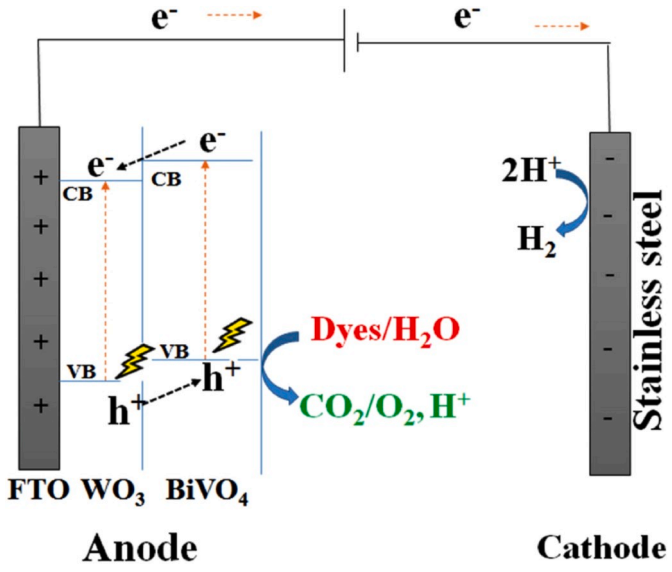

Fig. 11. Schematic diagram of FTO/WO_3/$BiVO_4$ photoanode electrode for dyes degradation under the photoelectrocatalytic mechanism.

visible light absorption, and better morphological properties cause photoelectrocatalytic activity improvement compared to those prepared by the previous spin coating method. We can confirm that the developed electrode preparation technique is simple, convenient, and suitable for scaling up applications. Under the optimum conditions, the designed PEC/solar cell can eliminate up to 94% of MB and 93% of RhB in 3 h and can reduce COD by up to 82% in 3 h, which confirms that the developed system is highly effective in treating dye wastewater. In particular, including solar cells and batteries with the PEC cell can reduce energy consumption and allow it to work independently, which is suitable for further development in the dye wastewater industry.

Declaration of competing interest

We have no conflict of interest to declare.

CRediT authorship contribution statement

Watcharapong Nareejun: Formal analysis, Data curation, Writing - original draft. **Chatchai Ponchio:** Formal analysis, Data curation, Writing - original draft.

Acknowledgement

This work was supported by the Research and Researchers for Industries (RRI) project, the Thailand Research Fund (TRF), and STP Chem Solutions Co., Ltd. (MSD59I0017). The authors also thank the Analysis and Instrumentation Center of Nagaoka University of Technology (Japan) for their support in the use of characterization instruments.

Appendix A. Supplementary data

Supplementary data to this article can be found online at https://doi.org/10.1016/j.solmat.2020.110556.

References

[1] B. Yang, H. Xu, S. Yang, S. Bi, F. Li, C. Shen, C. Ma, Q. Tian, J. Liu, X. Song, W. Sand, Y. Liu, Treatment of industrial dyeing wastewater with a pilot-scale strengthened circulation anaerobic reactor, Bioresour. Technol. 264 (2018) 154–162.
[2] J.K.H. Wong, H.K. Tan, S.Y. Lau, P.-S. Yap, M.K. Danquah, Potential and challenges of enzyme incorporated nanotechnology in dye wastewater treatment: a review, J. Environ. Chem. Eng. 7 (2019), 103261.
[3] T. Salinas, I. Durruty, L. Arciniegas, G. Pasquevich, M. Lanfranconi, I. Orsi, V. Alvarez, S. Bonanni, Design and testing of a pilot scale magnetic separator for the treatment of textile dyeing wastewater, J. Environ. Manag. 218 (2018) 562–568.
[4] K.K. Paul, N. Sreekanth, R.K. Biroju, T.N. Narayanan, P.K. Giri, Solar light driven photoelectrocatalytic hydrogen evolution and dye degradation by metal-free few-layer MoS_2 nanoflower/TiO_2 (B) nanobelts heterostructure, Sol. Energy Mater. Sol. Cell. 185 (2018) 364–374.
[5] E. Abroshan, S. Farhadi, A. Zabardasti, Novel magnetically separable Ag_3PO_4/$MnFe_2O_4$ nanocomposite and its high photocatalytic degradation performance for organic dyes under solar-light irradiation, Sol. Energy Mater. Sol. Cell. 178 (2018) 154–163.
[6] Y. Wei, Q. Ji, L. Chen, J. Hao, C. Yao, X. Dong, Preparation of an inorganic coagulant-polysilicate–magnesium for dyeing wastewater treatment: effect of acid medium on the characterization and coagulation performance, J. Taiwan Inst. Chem. Eng. 72 (2017) 142–148.
[7] A.S. Fajardo, R.C. Martins, D.R. Silva, C.A. Martínez-Huitle, R.M. Quinta-Ferreira, Dye wastewaters treatment using batch and recirculation flow electrocoagulation systems, J. Electroanal. Chem. 801 (2017) 30–37.
[8] J. Sarasa, M.P. Roche, M.P. Ormad, E. Gimeno, A. Puig, J.L. Ovelleiro, Treatment of a wastewater resulting from dyes manufacturing with ozone and chemical coagulation, Water Res. 32 (1998) 2721–2727.
[9] K. Rambabu, G. Bharath, P. Monash, S. Velu, F. Banat, M. Naushad, G. Arthanareeswaran, P. Loke Show, Effective treatment of dye polluted wastewater using nanoporous $CaCl_2$ modified polyethersulfone membrane, Process Saf. Environ. Protect. 124 (2019) 266–278.
[10] F. Li, J. Huang, Q. Xia, M. Lou, B. Yang, Q. Tian, Y. Liu, Direct contact membrane distillation for the treatment of industrial dyeing wastewater and characteristic pollutants, Separ. Purif. Technol. 195 (2018) 83–91.
[11] G. Gnanapragasam, M. Senthilkumar, V. Arutchelvan, T. Velayutham, S. Nagarajan, Bio-kinetic analysis on treatment of textile dye wastewater using anaerobic batch reactor, Bioresour. Technol. 102 (2011) 627–632.
[12] W.-L. Wang, Y.-Z. Cai, H.-Y. Hu, J. Chen, J. Wang, G. Xue, Q.-Y. Wu, Advanced treatment of bio-treated dyeing and finishing wastewater using ozone-biological activated carbon: a study on the synergistic effects, Chem. Eng. J. 359 (2019) 168–175.
[13] S.V. Mohite, V.V. Ganbavle, K.Y. Rajpure, Photoelectrochemical performance and photoelectrocatalytic degradation of organic compounds using Ga:WO_3 thin films, J. Photochem. Photobiol. Chem. 344 (2017) 56–63.
[14] M. Karimi-Nazarabad, E.K. Goharshadi, Highly efficient photocatalytic and photoelectrocatalytic activity of solar light driven WO_3/g-C_3N_4 nanocomposite, Sol. Energy Mater. Sol. Cell. 160 (2017) 484–493.
[15] W. Wang, F. Li, D. Zhang, D.Y.C. Leung, G. Li, Photoelectrocatalytic hydrogen generation and simultaneous degradation of organic pollutant via CdSe/TiO_2 nanotube arrays, Appl. Surf. Sci. 362 (2016) 490–497.
[16] P. Chatchai, A.Y. Nosaka, Y. Nosaka, Photoelectrocatalytic performance of WO_3/$BiVO_4$ toward the dye degradation, Electrochim. Acta 94 (2013) 314–319.
[17] W. Fei, Y. Song, N. Li, D. Chen, Q. Xu, H. Li, J. He, J. Lu, Fabrication of visible-light-active ZnO/ZnFe-LDH heterojunction on Ni foam for pollutants removal with enhanced photoelectrocatalytic performance, Sol. Energy 188 (2019) 593–602.

[18] X. Wang, Q. Wu, H. Ma, C. Ma, Z. Yu, Y. Fu, X. Dong, Fabrication of PbO_2 tipped Co_3O_4 nanowires for efficient photoelectrochemical decolorization of dye (reactive brilliant blue KN-R) wastewater, Sol. Energy Mater. Sol. Cell. 191 (2019) 381–388.
[19] N. Kangkun, N. Kiama, N. Saito, C. Ponchio, Optical properties and photoelectrocatalytic activities improvement of WO_3 thin film fabricated by fixed-potential deposition method, Optik 198 (2019), 163235.
[20] R. Yang, Y. Ji, Q. Li, Z. Zhao, R. Zhang, L. Liang, F. Liu, Y. Chen, S. Han, X. Yu, H. Liu, Ultrafine Si nanowires/Sn_3O_4 nanosheets 3D hierarchical heterostructured array as a photoanode with high-efficient photoelectrocatalytic performance, Appl. Catal. B Environ. 256 (2019), 117798.
[21] X. Cui, H. Gu, Y. Guan, G. Ren, Z. Ma, Y. Yin, J. Liu, X. Cui, L. Yao, Y. Yin, D. Wang, G. Jin, S. Rong, L. Tong, J. Hou, M. Li, Fabrication of $AgInS_2$ nanoparticles sensitized TiO_2 nanotube arrays and their photoelectrochemical properties, Sol. Energy Mater. Sol. Cell. 137 (2015) 101–106.
[22] S.S. Patil, M.A. Johar, M.A. Hassan, D.R. Patil, S.-W. Ryu, Enhanced photoelectrocatalytic water oxidation using CoPi modified GaN/MWCNTs composite photoanodes, Sol. Energy 178 (2019) 125–132.
[23] M. Lashgari, N. Shafizadeh, P. Zeinalkhani, A nanocomposite p-type semiconductor film for possible application in solar cells: photo-electrochemical studies, Sol. Energy Mater. Sol. Cell. 137 (2015) 274–279.
[24] X. Long, Q. Pan, C. Wang, H. Wang, H. Li, X. Li, Microbial fuel cell-photoelectrocatalytic cell combined system for the removal of azo dye wastewater, Bioresour. Technol. 244 (2017) 182–191.
[25] G.G. Bessegato, L.C. de Almeida, S.L.C. Ferreira, M.V.B. Zanoni, Experimental design as a tool for parameter optimization of photoelectrocatalytic degradation of a textile dye, J. Environ. Chem. Eng. 7 (2019), 103264.
[26] S. Xiao, D. Wan, K. Zhang, H. Qu, J. Peng, Enhanced photoelectrocatalytic degradation of ammonia by in situ photoelectrogenerated active chlorine on TiO_2 nanotube electrodes, J. Environ. Sci. 50 (2016) 103–108.
[27] J. Wu, H. Xu, W. Yan, Photoelectrocatalytic degradation Rhodamine B over highly ordered TiO_2 nanotube arrays photoelectrode, Appl. Surf. Sci. 386 (2016) 1–13.
[28] X. Zhang, L.-c. Nengzi, B. Li, L. Liu, X. Cheng, Design and construction of a highly efficient photoelectrocatalytic system based on dual-Pd/TNAs photoelectrodes for elimination of triclosan, Separ. Purif. Technol. 235 (2020), 116232.
[29] Q. Wang, Q. Yuan, Z. Liu, R. Jin, Y. Cui, S. Gao, Ultrasound-assisted synthesis and solar-light-driven photoelectrocatalytic activity of CdS sensitized TiO_2 nanotube array photocatalysts, Separ. Purif. Technol. 194 (2018) 216–221.
[30] X. Bai, L. Ma, Z. Dai, H. Shi, Electrochemical synthesis of p-Cu_2O/n-TiO_2 heterojunction electrode with enhanced photoelectrocatalytic activity, Mater. Sci. Semicond. Process. 74 (2018) 319–328.
[31] Q. Wang, R. Jin, C. Yin, M. Wang, J. Wang, S. Gao, Photoelectrocatalytic removal of dye and Cr(VI) pollutants with Ag_2S and Bi_2S_3 co-sensitized TiO_2 nanotube arrays under solar irradiation, Separ. Purif. Technol. 172 (2017) 303–309.
[32] Y. Wu, Y. Wei, Q. Guo, H. Xu, L. Gu, F. Huang, D. Luo, Y. Huang, L. Fan, J. Wu, Solvothermal fabrication of La-WO_3/$SrTiO_3$ heterojunction with high photocatalytic performance under visible light irradiation, Sol. Energy Mater. Sol. Cell. 176 (2018) 230–238.
[33] F. Li, W. Zhao, D.Y.C. Leung, Enhanced photoelectrocatalytic hydrogen production via Bi/$BiVO_4$ photoanode under visible light irradiation, Appl. Catal. B Environ. 258 (2019), 117954.
[34] Y.M. Hunge, A.A. Yadav, M.A. Mahadik, V.L. Mathe, C.H. Bhosale, A highly efficient visible-light responsive sprayed WO_3/FTO photoanode for photoelectrocatalytic degradation of brilliant blue, J. Taiwan Inst. Chem. Eng. 85 (2018) 273–281.
[35] J. Nong, G. Lan, W. Jin, P. Luo, C. Guo, X. Tang, Z. Zang, W. Wei, Eco-friendly and high-performance photoelectrochemical anode based on AgInS2 quantum dots embedded in 3D graphene nanowalls, J. Mater. Chem. C 7 (2019) 9830–9839.
[36] H. Du, W. Pu, Y. Wang, K. Yan, J. Feng, J. Zhang, C. Yang, J. Gong, Synthesis of $BiVO_4$/WO_3 composite film for highly efficient visible light induced photoelectrocatalytic oxidation of norfloxacin, J. Alloys Compd. 787 (2019) 284–294.
[37] B.O. Orimolade, B.A. Koiki, G.M. Peleyeju, O.A. Arotiba, Visible light driven photoelectrocatalysis on a FTO/$BiVO_4$/BiOI anode for water treatment involving emerging pharmaceutical pollutants, Electrochim. Acta 307 (2019) 285–292.
[38] P. Chatchai, S.-y. Kishioka, Y. Murakami, A.Y. Nosaka, Y. Nosaka, Enhanced photoelectrocatalytic activity of FTO/WO_3/$BiVO_4$ electrode modified with gold nanoparticles for water oxidation under visible light irradiation, Electrochim. Acta 55 (2010) 592–596.
[39] S.V. Mohite, V.V. Ganbavle, K.Y. Rajpure, Photoelectrocatalytic activity of immobilized Yb doped WO_3 photocatalyst for degradation of methyl orange dye, Journal of Energy Chemistry 26 (2017) 440–447.
[40] N. Iqbal, I. Khan, Z.H.A. Yamani, A. Qurashi, A facile one-step strategy for in-situ fabrication of WO_3-$BiVO_4$ nanoarrays for solar-driven photoelectrochemical water splitting applications, Sol. Energy 144 (2017) 604–611.
[41] P. Chatchai, Y. Murakami, S.-y. Kishioka, A.Y. Nosaka, Y. Nosaka, Efficient photocatalytic activity of water oxidation over WO_3/$BiVO_4$ composite under visible light irradiation, Electrochim. Acta 54 (2009) 1147–1152.
[42] A. El Haimeur, M. Makha, H. Bakkali, J.M. González-Leal, E. Blanco, M. Dominguez, Z.V. Voitenko, Enhanced performance of planar perovskite solar cells using dip-coated TiO_2 as electron transporting layer, Sol. Energy 195 (2020) 475–482.
[43] Z. Wei, F. Liang, Y. Liu, W. Luo, J. Wang, W. Yao, Y. Zhu, Photoelectrocatalytic degradation of phenol-containing wastewater by TiO_2/g-C_3N_4 hybrid heterostructure thin film, Appl. Catal. B Environ. 201 (2017) 600–606.
[44] B. Zhou, J. Qu, X. Zhao, H. Liu, Fabrication and photoelectrocatalytic properties of nanocrystalline monoclinic $BiVO_4$ thin-film electrode, J. Environ. Sci. 23 (2011) 151–159.
[45] B. Yang, M. Wang, X. Hu, T. Zhou, Z. Zang, Highly efficient semitransparent $CsPbIBr_2$ perovskite solar cells via low-temperature processed In_2S_3 as electron-transport-layer, Nano Energy 57 (2019) 718–727.
[46] Y. Xu, J. Jia, D. Zhong, Y. Wang, Degradation of dye wastewater in a thin-film photoelectrocatalytic (PEC) reactor with slant-placed TiO_2/Ti anode, Chem. Eng. J. 150 (2009) 302–307.
[47] M. Patel, W.-H. Park, A. Ray, J. Kim, J.-H. Lee, Photoelectrocatalytic sea water splitting using Kirkendall diffusion grown functional Co_3O_4 film, Sol. Energy Mater. Sol. Cell. 171 (2017) 267–274.
[48] M. Shang, W. Wang, L. Zhou, S. Sun, W. Yin, Nanosized $BiVO_4$ with high visible-light-induced photocatalytic activity: ultrasonic-assisted synthesis and protective effect of surfactant, J. Hazard Mater. 172 (2009) 338–344.
[49] Š. Paušová, M.U. Gray, M. Neumann-Spallart, J. Krýsa, Photoelectrochemical properties of $BiVO_4$ thin film photoanodes prepared by aerosol pyrolysis, Catal. Today 326 (2019) 30–35.
[50] C. Wang, M. Wu, M. Yan, H. Shen, F. Cai, B. Hu, W. Shi, Enhanced visible-light photocatalytic activity and the mechanism study of WO_3 nanosheets coupled with Ag_3PO_4 nanocrystals, Ceram. Int. 41 (2015) 6784–6792.
[51] F. Guo, W. Shi, X. Lin, G. Che, Hydrothermal synthesis of graphitic carbon nitride–$BiVO_4$ composites with enhanced visible light photocatalytic activities and the mechanism study, J. Phys. Chem. Solid. 75 (2014) 1217–1222.
[52] L. Ji, B. Liu, Y. Qian, Q. Yang, P. Gao, Enhanced Visible-Light-Induced Photocatalytic Disinfection of Escherichia coli by Ternary Bi_2WO_6/TiO_2/reduced Graphene Oxide Composite Materials: Insight into the Underlying Mechanism, Advanced Powder Technology, 2019.
[53] H. Wang, B. Liao, T. Lu, Y. Ai, G. Liu, Enhanced visible-light photocatalytic degradation of tetracycline by a novel hollow BiOCl@CeO_2 heterostructured microspheres: structural characterization and reaction mechanism, J. Hazard Mater. 385 (2020), 121552.
[54] M. Long, W. Cai, J. Cai, B. Zhou, X. Chai, Y. Wu, Efficient photocatalytic degradation of phenol over Co_3O_4/$BiVO_4$ composite under visible light irradiation, J. Phys. Chem. B 110 (2006) 20211–20216.
[55] T. Peng, K. Fan, D. Zhao, J. Chen, Enhanced energy conversion efficiency of Mg2+-modified mesoporous TiO_2 nanoparticles electrodes for dye-sensitized solar cells, J. Phys. Chem. C 114 (2010) 22346–22351.
[56] J.N. Yao, P. Chen, A. Fujishima, Electrochromic behavior of electrodeposited tungsten oxide thin films, J. Electroanal. Chem. 406 (1996) 223–226.
[57] L. Ge, Novel Pd/$BiVO_4$ composite photocatalysts for efficient degradation of methyl orange under visible light irradiation, Mater. Chem. Phys. 107 (2008) 465–470.
[58] G. Leftheriotis, S. Papaefthimiou, P. Yianoulis, A. Siokou, Effect of the tungsten oxidation states in the thermal coloration and bleaching of amorphous WO_3 films, Thin Solid Films 384 (2001) 298–306.
[59] S.V. Mohite, V.V. Ganbavle, K.Y. Rajpure, Solar photoelectrocatalytic activities of rhodamine-B using sprayed WO_3 photoelectrode, J. Alloys Compd. 655 (2016) 106–113.
[60] N. Kiama, C. Ponchio, Photoelectrocatalytic performance improvement of $BiVO_4$ thin film fabrication via effecting of calcination temperature strategy, Surf. Coating. Technol. 383 (2020), 125257.
[61] D. Liu, R. Tian, J. Wang, E. Nie, X. Piao, X. Li, Z. Sun, Photoelectrocatalytic degradation of methylene blue using F doped TiO_2 photoelectrode under visible light irradiation, Chemosphere 185 (2017) 574–581.
[62] R.D. Suryavanshi, S.V. Mohite, A.A. Bagade, K.Y. Rajpure, Photoelectrocatalytic activity of spray deposited Fe_2O_3/ZnO photoelectrode for degradation of salicylic acid and methyl orange dye under solar radiation, Mater. Sci. Eng., B 248 (2019), 114386.